

Numerical simulation and experimental validation of the dip-coating process

Xian-Ming Zhang, Meng-Meng Chen, Jian-Ping Ma,
Wen-Xing Chen, and Lian-Fang Feng

A comprehensive investigation involved the direct measurement of the thickness, free surface, and flow field of non-Newtonian fluids and poly-acrylic acid solutions.

During the dip-coating process, a clean substrate is vertically withdrawn from a coating fluid at a constant speed, where the effects of fluid viscous force, surface tension, and gravity keep the fluid attached to the substrate. A uniform thin film is then deposited on the substrate after drying and curing. The products of this process are normally used as decorative and protective films, as well as in more functional applications (e.g., galvanized steel, magnetic information storage systems, and the manufacture of semiconductor components). The film flow that occurs during the coating process, however, is a typical interface flow that exhibits very complicated dynamic behavior and requires dedicated research.

Film flow during dip-coating has been the subject of several previous theoretical and experimental studies. For example, in a study of the film flow of Newtonian fluids with high capillary (Ca) and Reynolds (Re) numbers, it was shown that the final film thickening and free surface depended greatly on the Ca and Re.¹ In addition, it has been found² that surfactants and roughness can result in significant thickening of the coating film relative to the clean interface and smooth substrate case, but this film thickening was not the result of the Marangoni effect (i.e., mass transfer along an interface between two fluids caused by a surface tension gradient). These previous investigations of film flow, however, were somewhat simple in either their experimental or numerical scope.

In this work,³ we have thus conducted a more comprehensive and detailed investigation of the film-flow problem in dip-coating for non-Newtonian fluids. In our approach we directly measure the experimental film thickness and free surface so that we can analyze—both experimentally and numerically, under given conditions—the evolution of the liquid film thickness, free surface, and flow field of the fluids. We have also successfully compared our numerical and experimental

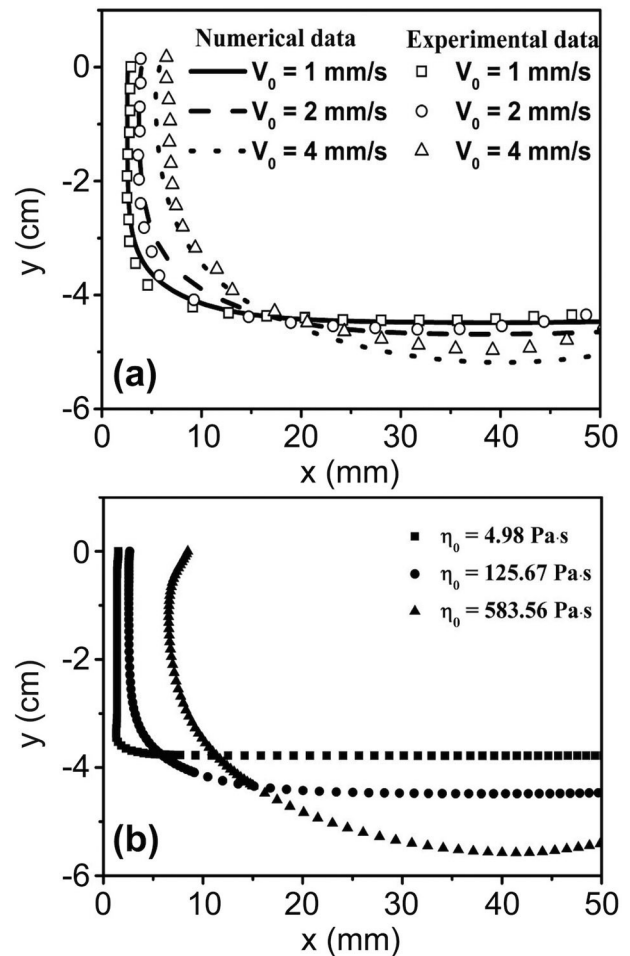


Figure 1. (a) Numerical simulation and experimental results, showing how changing the withdrawal velocity (V_0) affects the free surface (in the x and y dimensions) of silicone oil fluid C (see Table 1). (b) The effect (numerically obtained results) of changing the zero-shear viscosity (η_0) of the three silicone oil fluids (at $V_0 = 1$ mm/s).

Continued on next page

Table 1. Rheological and physical properties of silicone oil fluids and polyacrylic acid (PAA) solutions investigated in this study.

Silicone oil fluids	Density ρ (kg/m ³)	Surface tension σ (N/m)	Zero-shear viscosity η_0 (Pa · s)	Relaxtion time λ (s)	Non-Newtonian index n	
A	970	0.0212	0.97	—	—	
B	974	0.0213	4.98	0.03	0.70	
C	977	0.0215	125.67	0.15	0.71	
D	978	0.0216	583.56	0.08	0.53	
PAA solutions (mass fraction)	Density ρ (kg/m ³)	Surface tension σ (N/m)	Yield stress τ_0 (Pa)	Consistency factor K	Non-Newtonian index n	Critical shear rate $\dot{\gamma}_c$ (s ⁻¹)
0.3%	1014	0.104	3.20	20.32	0.76	0.001
0.4%	1020	0.147	9.40	84.88	0.77	0.003

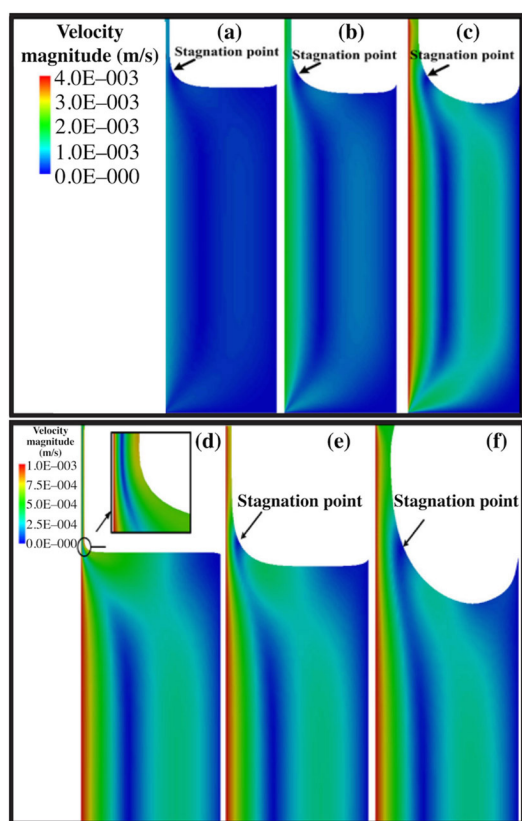


Figure 2. Flow field results showing the variation of the smooth surface of the norm-velocity field. Top: Results for silicone oil fluid C at V_0 of (a) 1mm/s, (b) 2mm/s, and (c) 4mm/s. Bottom: Results, at V_0 of 1mm/s, for (d) silicone oil fluid B, (e) silicone oil fluid C, and (f) silicone oil fluid D.

results. We base our numerical simulations on constitutive equations of non-Newtonian Carreau–Yasuda (CY) and Herschel–Bulkley (HB) fluids, and have used our models to focus particularly on the thickening of the coating film.

The rheological properties of the four silicone oil fluids (three of which are non-Newtonian)⁴ and the two polyacrylic acid (PAA) solutions that we studied are given in Table 1. These values show that the steady-state shear viscosities of the non-Newtonian silicone oil fluids (i.e., B, C, and D) and the PAA solutions are consistent with the CY and HB models. A CY fluid model is used when pseudo-plastic and Newtonian behavior is exhibited at high and low shear rates, respectively. In contrast, an HB model is applicable when the yield stress of a fluid does not exhibit noticeable viscoelastic effects.

The results of our numerical simulations and our experiments on CY fluids are shown in Figure 1(a) for the example of the silicone oil fluid C. The two sets of results are in good agreement for different withdrawal velocity (V_0) values, which verifies that fluid viscosity and V_0 are the most important influences on the free surface and the film thickness of the fluids. We also find that the film thickness for all three non-Newtonian silicone oil fluids significantly increased with increasing viscosity: see Figure 1(b). Stagnation occurs at the point where the velocity of the fluid is zero. As the distance between the stagnation point and the substrate increases, a large amount of fluid is dragged by the substrate and leads to thickening of the coating film. It is thus useful to analyze the variation of film thickness by examining the stagnation point position.

Our flow field results (see Figure 2) also demonstrate that the thickening of the coating film and the free surface level gradually decrease with increasing V_0 or viscosity. By comparing the flow fields shown in Figure 2(a–c) with previously obtained results,⁵ we predict that a stag-

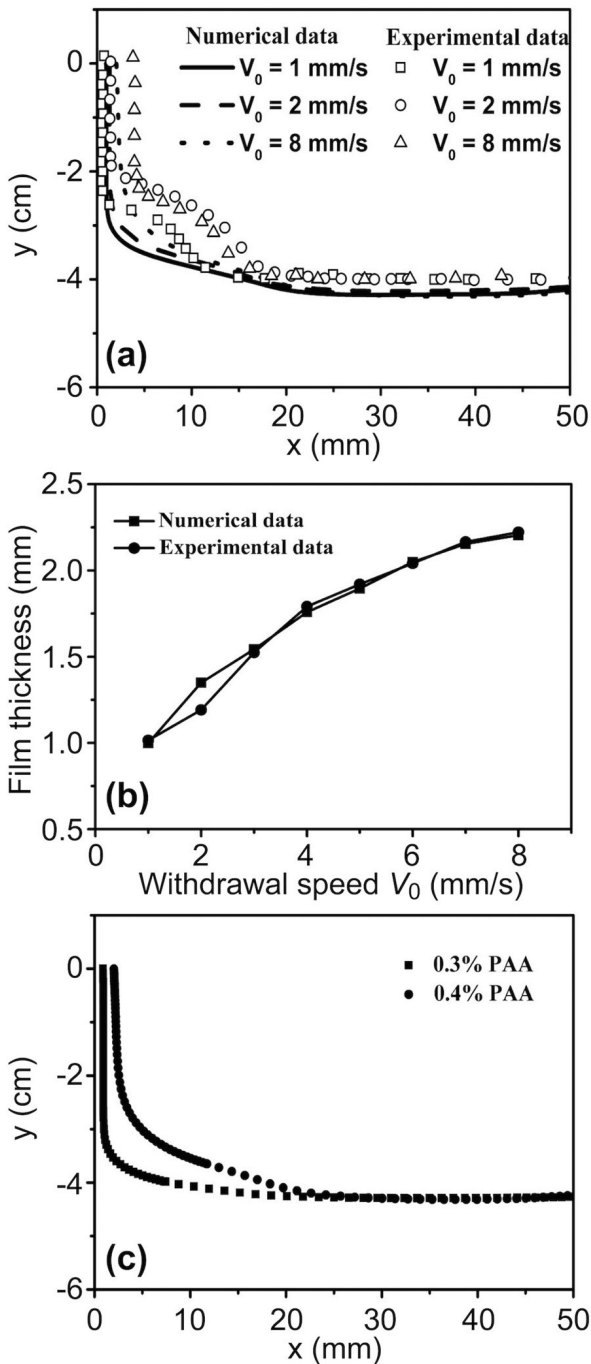


Figure 3. (a) Numerical and experimental results showing how changing V_0 affects the free surface of the 0.4% PAA solution. (b) Comparison of the numerically and experimentally obtained final film thickness results of the 0.4% PAA solution. (c) Numerical measurements of the free surface of the 0.3 and 0.4% PAA solutions (at V_0 of 8mm/s).

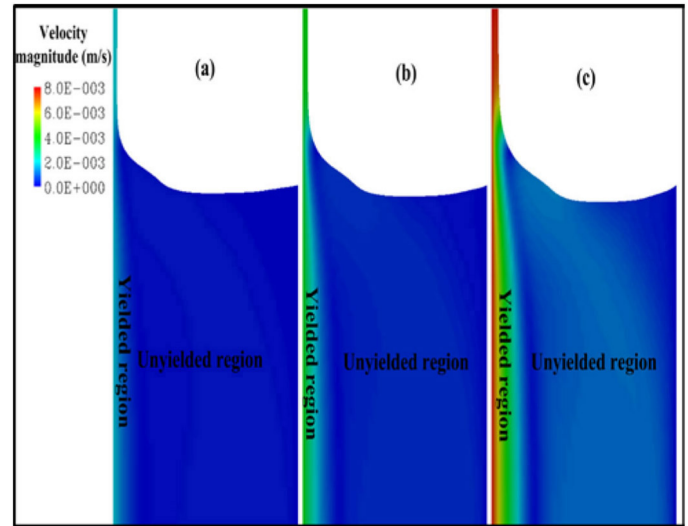


Figure 4. Flow fields that illustrate the yielded and unyielded stress regions in the 0.4% PAA solution for V_0 of (a) 2mm/s, (b) 4mm/s, and (c) 8mm/s.

nation point would occur on the free surface if the withdrawal speed were high enough. Furthermore, by comparing the flow field in Figure 2(d) with those in Figure 2(e) and (f), we observe that a stagnation point appears on the free surface when the viscosity is large enough. We have thus confirmed that a stagnation point on the free surface occurs with increasing withdrawal velocity or fluid viscosity.

For our examination of HB fluids, we conducted numerical simulations for two different mass fraction PAA solutions (0.3 and 0.4%) with different levels of yield stress. We find—see Figure 3(a)—that the entrainment of the free surface occurs only in the dynamic region and that a hump appears on the free surface. Although there is a discrepancy in the height of this hump between our numerical and experimental results (the experimental results suggest that it is much taller), the two final numerical film thickness data sets are in accordance: see Figure 3(b). The results in Figure 3(a) and (b) also reveal that by increasing V_0 , the final film thickness tends to increase, but the position of the liquid level cannot be modified. In addition, our results—see Figure 3(c)—show that the hump on the free surface is almost invisible for the 0.3% PAA solution, but that it is larger for the 0.4% solution. This demonstrates that increased yield stress favors the formation of the hump. For the 0.4% PAA solution, the shear stress increases as a function of the viscosity, yield stress, and entrainment of fluid along the plate substrate, which results in thickening of the film. Lastly, we present the norm-velocity (i.e., obtained from the post-processing software Fieldview) field for

the 0.4% PAA solution at a V_0 of 8mm/s in Figure 4. This field is similar to that of the silicone oil fluids (see Figure 2), but in this case we observe a hump located on the free surface. We also observe important changes in the velocity field that arise because of the presence of yield stress.

In summary, we have conducted numerical simulations of dip-coating with non-Newtonian fluids. We have also conducted equivalent experiments to verify our modeling results. We find that our numerical simulation methodology can successfully be used to provide detailed and quantitative information regarding the film thickness, free surface, and flow field (which are difficult to obtain using experimental methods). For many of the cases we examined, our numerical and experimental results are in good agreement. In the next stages of our research we will focus on the analysis of fluid mechanics in the dip-coating process, including the surface tension, gravity, and viscous forces. This analysis will help us to explain the effect of the forces on film flow characteristics and liquid film thickness.

Author Information

Xian-Ming Zhang, Meng-Meng Chen, Jian-Ping Ma, and Wen-Xing Chen

Zhejiang Sci-Tech University
Hangzhou, China

Lian-Fang Feng

Zhejiang University
Hangzhou, China

References

1. J. P. Kizito, Y. Kamotani, and S. Ostrach, *Experimental free coating flows at high capillary and Reynolds number*, **Experim. Fluids** **27**, pp. 235–243, 1999.
2. R. Krechetnikov and G. M. Homsy, *Surfactant effects in the Landau–Levich problem*, **J. Fluid Mech.** **559**, pp. 429–450, 2006.
3. X.-M. Zhang, M.-M. Chen, J.-P. Ma, W.-X. Chen, and L.-F. Feng, *Numerical simulation and experimental validation of liquid-film-flow characteristics in dip coating for non-Newtonian fluids*, **Polym. Eng. Sci.**, 2016. doi:10.1002/pen.24339
4. J. Boujlel and P. Coussot, *Measuring the surface tension of yield stress fluids*, **Soft Matter** **9**, pp. 5898–5908, 2013.
5. P. Hurez and P. A. Tanguy, *Finite element analysis of dip coating with Bingham fluids*, **Polym. Eng. Sci.** **30**, pp. 1125–1132, 1990.